Optimization of the Working Process of a Two-Stage HPT of a Modern GTE for Civil Aviation

Grigorii Popov[1]*, Vasilii Zubanov [1], Evgenii Goriachkin [1], Anastasia Shcherban [1], and Andrey Shvyrev [2]

[1] Samara National Research University, Samara, Russia; Email: popov@ssau.ru, waskes91@gmail.com, goriachkin.e.s@gmail.com, korneeva.ai@ssau.ru

[2] UEC Aviadvigatel, Perm, Russia; Email: shvyrev@avid.ru

*Correspondence: popov@ssau.ru

Abstract*— The paper describes an optimization process of an axial two-stage high-pressure turbine (HPT) of a gas turbine engine (GTE) for a civil aviation aircraft. This turbine was optimized to increase efficiency and reduce the output swirl gradient. The original turbine has a high efficiency so no significant improvement of efficiency was found using conventional approaches. A large number of variables must be used to describe the process, and the computational model, taking into account film cooling modeling, is time consuming and computationally intensive. In this regard, direct optimization did not provide a meaningful result. For this reason, a series of optimization problems were solved by varying the parameterization schemes, the number of variable sections, the grid of finite volumes and the degree of detailing of the mathematical model. During the optimization process, the issues of ensuring the strength and service life of the blades were not considered, however, the range of changes in the geometry of the blades was chosen in such a way as to prevent a significant deterioration in the strength parameters. As a result, 2 variants of optimization of turbine geometry have been found: the first variant in which only forms of control sections of blades (2D form) changed allowed to increase efficiency by 0.37 %. The second variant in which both shape of profiles and their mutual position relative to each other were changed (2D and 3D form) allowed to increase efficiency by 0.63% at significant decrease of gradient of the flow exit angle.

***Keywords* —axial turbine, numerical simulation, optimization, parametrization, cooling, 3D profiling**

I. Nomenclature

$\pi_T{}^*$	gas expansion ratio in the turbine;
α_{exit}	turbine flow exit angle.
GTE	gas turbine engine;
HPT	high pressure turbine;
NGV	nozzle guide vane;
RW	rotor wheel;
ER	Mesh cells Expansion ratio;
MR	Mesh cell maximum aspect ratio.

Manuscript received July 28, 2022; revised December 5, 2022; accepted December 25, 2022.

II. Introduction

Modern turbines in gas turbine aircraft engines operate at high inlet gas temperatures. This can reach up to 2000K. This temperature exceeds the melting point of blade materials and the blades are cooled intensively to ensure their performance [1, 2]. Nowadays open cooling systems are applied in turbines where the turbine is cooled by "cold air". It flows through the internal channels of the blade and comes out to the flow path through the holes on the surface of the blade or near the trailing edge.

Blowing coolant into the flow path significantly changes the flow pattern in the channels. For the qualitative design of new and upgraded cooled turbines, the interaction process between the main flow and the coolant jets must be modelled. Currently, there are several approaches to such modeling.

The cooling air supply system can be modeled separately to determine the values of the air parameters at the inlet to the internal cavities of the blades [3]. These values are the boundary conditions for modeling the internal cavities of the blades with perforation channels in the walls of the blades and the tract shelves of guide vanes [4, 5]. Optimization of the shape of the channels and the internal cavity in modeling the internal cavities of blades with perforation channels can be performed in order to increase cooling efficiency, as for example in [6,7].

However, with computational fluid dynamic (CFD) modelling this would lead to a significant increase in the size of the model and would be resource-intensive and time-consuming to compute. As a result, the time for finding a design solution would increase significantly up to unacceptable values. The use of mathematical optimization methods in this case would also not be effective, as their application requires thousands of runs to the calculation model, which will also require a huge amount of time At the same time, for uncooled turbines, good results have been obtained in many works to increase efficiency by optimizing the shapes of the blades

doi: 10.18178/ijmerr.12.1.48-56

and the flow part. Examples of optimization of uncooled turbines are given in [8, 9].

Despite the complexity of the optimization of cooled turbines using CFD models, the authors nevertheless aimed to optimize the two-stage cooled turbine developed at UEC Aviadvigatel [10]. The turbine has gas expansion ratio equal to π_{T*}=4.76. Fig. 1 shows relative flow rates of cooling air at the turbine inlet relative to the flow rate at the inlet to the first nozzle guide vane (NGV) of the turbine.

In order to reduce the time of reference to the mathematical model and the time for obtaining the solution as a whole, a simplified numerical model was used, in which the internal channels of the blade cooling system are not modelled, and the coolant discharge is modelled as point sources of mass flow rate. In this case the mesh size is practically not increased in comparison with the model without cooling and the preparation time of the numerical model is considerably reduced. Such models are useful in the design and computational development phases when multiple turbine variants need to be calculated and compared.

III. Numerical Turbine Model

A numerical model of the turbine working process was created with Numeca Fine/Turbo (Fig. 2).

Modelling was performed in the stationary formulation with the condition of cyclic symmetry. The model takes into account the presence of an inter-disk cavity between the NGV and the rotor wheel (RW) of the 1st stage, as well as the cavity of the labyrinth seal under the NGV of the 2nd stage. Radial clearance on the turbine blades is considered in the model.

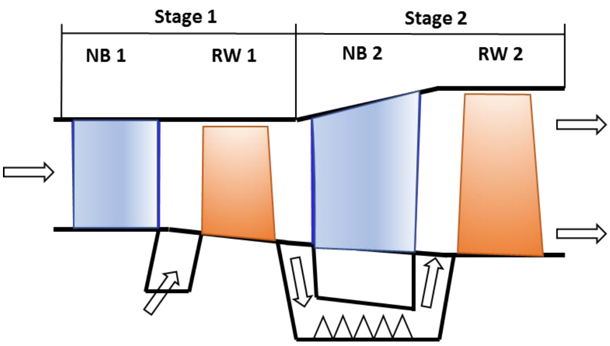

Figure 1. Flow path diagram of the turbine in question.

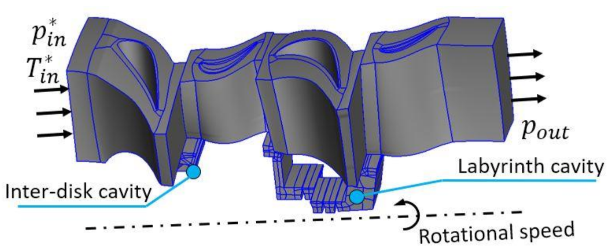

Figure 2. Numerical model of the turbine working process.

An ideal gas with combustion product properties of kerosene was used as the working fluid. Turbulence model is Spalart-Allmaras. The turbulence model was chosen based on the positive experience of its application in the problems of studying and optimizing the working process of turbines [11]. According to our experience, it is the best in terms of accuracy / consumed resources. The last circumstance is especially important when solving optimization problems. The maximum value of Y+ did not exceed 5.

At the turbine inlet, the average values of total pressure and temperature have been set. The direction of the flow angle at the turbine inlet is axial. At the turbine outlet the static pressure at the hub radius was set. Pressures at other radiuses were calculated by radial equilibrium equation. Static pressure value at the turbine outlet was set according to required total pressure ratio. For data transfer between the NGV and RW areas, a Full Non Matching Mixing Plane type interface was used in the Numeca Fine/Turbo software package.

Modelling of cooling air discharge was performed by blowing additional working fluid out of the calculation grid cells, see Fig. 3.

Positioning of cooling air exhaust rows was performed in relative terms by variables Bi, Rhi and Rsi, where Bi is the relative coordinate of the i-th cooling air exhaust row along the blade surface; Rhi and Rsi are the relative height at which the i-th cool-ing air exhaust row starts and ends respectively.

Angles of direction of cooling air blows were set relative to the surface of the de-sign grid at the hole locations.

This numerical model has been validated against the experimental data provided by Aviadvigatel. The settings were found to provide low computer resource require-ments but still give a good agreement with the experimental data.

In the course of research, it was found that the created numerical model allows to find turbine capacity with an accuracy of 0.5%, efficiency with an accuracy of 1.5%, values of total pressure and temperature in the flow path with an accuracy of not less than 2%. It is established that in order to achieve such parameters the number of elements in one layer of finite volume mesh (B2B mesh) must be 10 thousand, mesh cell maximum aspect ratio (MR) criterion value for the mesh must be at least 1000, mesh cells Expansion ratio (ER) criterion equal to 1.2.

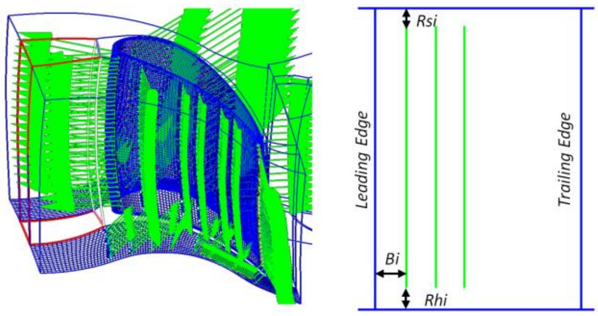

Figure 3. Description of Cooling Air Exhaust from the Computational Grid Cells.

The reasons for choosing these grid settings are given in the article GPPS-TC-2022-0057 prepared for this conference, which is the first stage of this work. This mesh, although coarse, is sufficient to obtain reliable results. The difference between the data obtained with its help, relative to the dense grid data will not exceed 0.05% with a significant reduction in the required computer resources.

IV. Optimization Strategy

The optimization was carried out using the IOSO software [12]. It is based on an optimization method using a response surface, which is refined and evolves each time the computational model is accessed. Each IOSO iteration contains two steps. In the first step, a response function in the form of a multi-level graph is constructed based on early model accesses with different combinations of varying variables. The next step is to search for an extremum of the found function. This approach makes it possible to constantly adjust the response surface in the process of optimization. As a result, an unusually small number of initial points are required to start the optimization process in order to construct it and get the first results [13-14].

An important advantage of IOSO is that this algorithm has low sensitivity to the topology of the target functions and allows one to successfully solve problems for smooth, modal, and undifferentiated functions. This allows the researcher not to think about mathematical features of the problem to be solved and to be confident in the correctness of the solution obtained. The convergence speed of IOSO optimisation algorithms is comparable to the fastest gradient algorithms for smooth unimodal functions and exceeds all known methods for complex functions. This makes it possible to solve optimisation problems at an acceptable time cost even when the time per calculation is several hours and the number of independent variables can exceed a hundred [4].

An important factor that influenced the choice of IOSO as the optimiser for the task at hand was the large number of positive examples of its use specifically in the field of turbomachinery performance improvement [12, 15-17].

The first attempt to solve the optimisation problem in a similar way as the authors did in previous studies was unsuccessful [18]. The initial geometry of the turbine had high efficiency and the found benefit was insignificant.

For this reason, further optimisation was solved in several steps. During these steps the influence of schemes of parameterization of shapes and mutual position of sections of blades of NGV and RW, and also consideration or neglection of inter-disk cavities on the achieved results was investigated.

The optimisation scheme and their interrelationships are shown in Table I. As can be seen, it was conducted in several steps. The results of the previous step served as a starting point for the search for an optimum in the next step.

TABLE 1. Steps in Solving Optimisation Tasks.

Step 1

Variant	1.1	1.2	1.3	1.4
Number of variable stator cross sections	3	3	5	5
Rotor chord	No changes			
Thickness of the NGV changes	No	Yes	No	No
Number of variables	43	91	59	59
Parameterisation method	*Legasy*			
Finite volume size	Small 19.000 cells per layer		Large 27.000 cells per layer	
Inter-disk cavity	No Consider			

Step 2

Variant	2.1	2.2	2.3	2.4	2.5
Number of variable stator cross sections	3	3	5	3	5
Rotor chord	Yes changes				
Thickness of the stator blade changes	Yes				
Thickness of the rotor blade changes	Yes	Yes	No	No	Yes
Number of variables	145	145	145	97	193
Parameterisation method	*Legasy*		*Throat_Base*		*Legasy*
Finite volume size	Small 19.000 cells per layer				
Consideration of the inter-disk cavity	No	Yes	No	No	No

Step 3

Variant	3.1	3.2
Number of variable stator cross sections	5	
Rotor chord changes	Yes	
Thickness of the stator blade changes	No	
Thickness of the rotor blade changes	No	
Number of variables	193	193
Finite volume size	Small 19.000 cells per layer	
Consideration of the inter-disk cavity	No	
Blade profile position parameterisation scheme	Variant 1 (figure 13)	Variant 2 (figure 13)

At the first step, two-dimensional blade re-profiling was carried out according to the criteria of increasing efficiency and decreasing the average integral value of the turbine's flow exit angle. Also at this step, the influence of the NGV and RW parameterisation schemes and the influence of the number of elements in the design grid were considered.

At the second step, a two-dimensional re-profiling of the blades was carried out according to the criteria of increasing the efficiency and decreasing the height gradient of the turbine's flow exit angle. In addition, at this step, the influence of the parameterization method and the feasibility of considering the labyrinth seal cavity in the computational grid were investigated. Based on the results of the second step, the final formulation of the 2D blades re-profiling problem was formed, including the most general parameterization scheme and the best versions of the previous tasks (as starting search points).

The third step involved a three-dimensional re-profiling of the blades using two different ways of parameterizing the mutual position of the sections in the axial and circumferential directions.

V. General Formulation of Optimization Problems

A. Optimization Task Criteria

All the optimization tasks were two-criteria. The first criterion was common to all steps - the turbine efficiency was to be increased as much as possible.

The second criterion of the optimization varied at different steps. In the first step, the average value of the flow exit angle from the turbine was to be reduced.

At the second and third steps, the second criterion was to reduce the radial gradient of the turbine's exit angle.

As a result of solving optimization problems Pareto fronts of optimal solutions were formed.

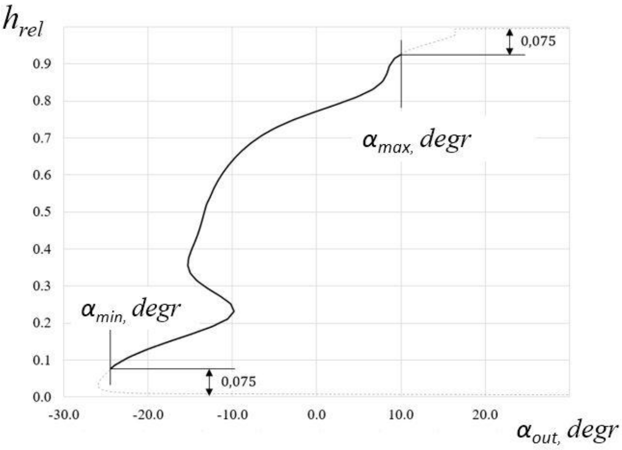

Figure 4. Schematic Diagram for Determining the Turbine Exit Angle Gradient.

The diagram for determining the exit angle gradient is shown in Fig. 4. The turbine exit gradient $\Delta\alpha exit$ by height is defined as the difference between the maximum αmax and minimum αmin by height of the turbine exit gradient. These values were deter-mined from the distribution graph of the circumferentially averaged flow exit angle in the turbine outlet section. Areas of near-wall flows with a large exit angle gradient were not considered in the analysis. For this purpose, the flow exit angle analysis was performed for relative heights between 0.075 and 0.925.

B. Varying Parameters of the Optimization Tasks

The variables defining the shape of the blades in their parametric models were used as varying parameters. The blades were parameterized in the NUMECA AutoBlade software. In all tasks, the Legasy parameterization scheme shown in Fig. 5 was used to describe the shape of the NGV and RW blade sections with cylindrical sections (except for variant 2.4). In this approach, the centre line of each cross section was described by four variables (chord, blade inlet and outlet angles and stagger angle) and the blade profile by eight (radii of leading and trailing edges, sharpening of the trailing edge and normal distance from the centre line of the five spline control points describing the suction and pressure sides).

In task 2.4, a different NGV parameterization scheme was used, see Table I, compared to the other tasks, based on the Throat_Base parameterization method in which the throat and effective flow angle are specified, see Fig 6. The description of the centre line is identical to the previous method. The blade profile is described by eleven variables (radii of leading and trailing edges, edge sharpening, throat, effective outlet angle and normal distance from the centre line of the three spline control points describing the suction and pressure sides).

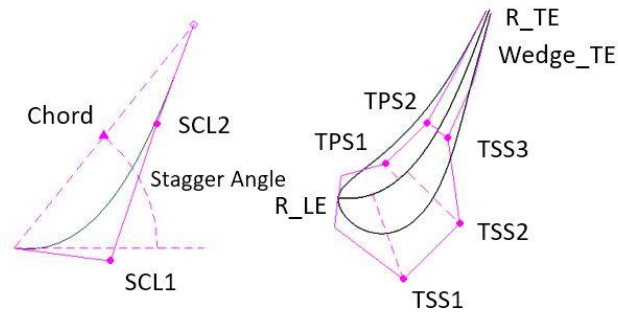

Figure 5. Blade parameterization diagram for optimization (legasy) [18].

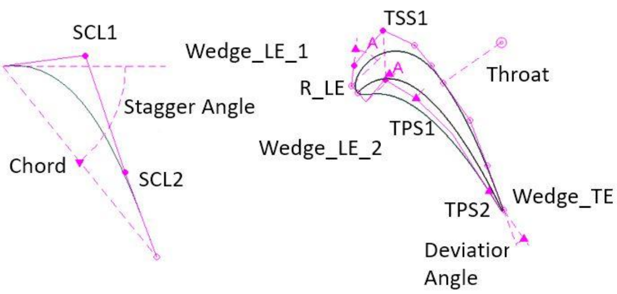

Figure 6. Blade parameterization diagram for optimization (throat_base) [18].

VI. Solving the Optimization Problems of Step 1

The first step was to modify the blade profiles. In total four optimization problems were created (1.1...1.4), see Table I. They differed in the number of sections to be changed, size of finite volume mesh and change of blade thicknesses.

For each optimization problem of step 1 at least 5000 calls of the optimizer to the solver were performed. As a result, the Pareto fronts of the optimization problems were generated, see Fig. 7.

From the results of step 1 of the optimization presented in Fig. 7, it can be seen that the use of increased density of finite volumes in the computational grid of the optimization numerical model of the HPT working process is inexpedient. Since this results in a significant increase in the time per call, but no significant difference in the achieved optimization results compared to low-density finite-volume meshes. This can be seen from the comparison of the Pareto front of variant 1.4 with variants 1.1 - 1.3, see Table I.

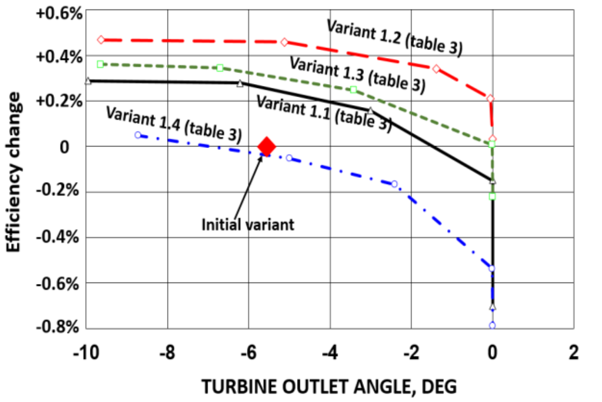

Figure 7. Comparison of the Pareto fronts of step 1 optimization problems.

Additional modification of the NGV thicknesses (task 1.2, shown in Table I) resulted in a maximum efficiency of 0.1% higher than in the task without modification of the NGV thicknesses (task 1.1, shown in Table I).

Application of five parametric sections of NGV (task 1.3, shown in Table I) resulted in maximum efficiency by 0.07% more than in application of three parametric sections of NGV (task 1.1, shown in Table I).

Thus, it is reasonable to use the scheme of parameterization with five parametric sections of NGV and varying thicknesses of NGV blade profiles.

VII. Solving the Optimization Problems of Step 2

The optimization problems of the second step were created on the basis of the optimization problems of the first step. At this stage the optimization criterion was changed, chord and thickness of rotor and stator blades were varied, and the inter-disk cavities were taken into account. Pareto fronts obtained as a result of 2nd step optimization problems are shown in Fig. 8.

It can be seen from Fig. 8 that application of the Throat_Base blades parameterization scheme (task 2.4, shown in Tab. 1) resulted in solutions which have worse efficiency in comparison with those obtained in the tasks with the Legacy parameterization scheme. Therefore, application of the Throat_Base blade parametrization method in the future was considered inexpedient.

The task in which the mathematical model took into account the presence of inter-disk cavities (task 2.2, shown in Table I) showed a smaller increase in the efficiency of the HPT than in the tasks without taking into account the cavities in the computational grid. Besides, the account of inter-disk cavities in calculation grid imposes restrictions on change of blades geometry (at some combinations of geometrical parameters of blades the near-tract cavities and flow path are not coupled correctly because of intersection of their elements), requires large computational resources and makes numerical solution less stable (probably because of a presence of tear areas in inter-disk cavities or incorrect mesh creation in a junction of a flow path and near-tract cavities). As a result, it is not possible to calculate all combinations of input data, making it difficult to find the optimum and increasing the number of calls to the computational model. Therefore, the use of a computational mesh with trap cavities in the HPT optimization numerical model was considered inappropriate.

Parametrization of NGV blades in five sections (task 2.3, shown in Table I) allowed to obtain maximum efficiency by 0.05% more than when three parametrized NGV sections were applied (task 2.1, shown in Table 1).

Optimization problem 2.5, see Tab. 1, is the most general 2D HPT re-profiling problem. It included the most common parametrization scheme with five parametrizable sections of NGV and three variable sections of RW with changing thicknesses of NGV and RW blades profiles. No additional restrictions were applied to change the thickness.

When starting the optimization process of variant 2.5, see Table I, the Pareto fronts obtained by solving other optimization variants were used as starting points. In addition, in this formulation a new constraint was added, which eliminated the variants with a gradient of change of the flow exit angle greater than that of the original turbine variant.

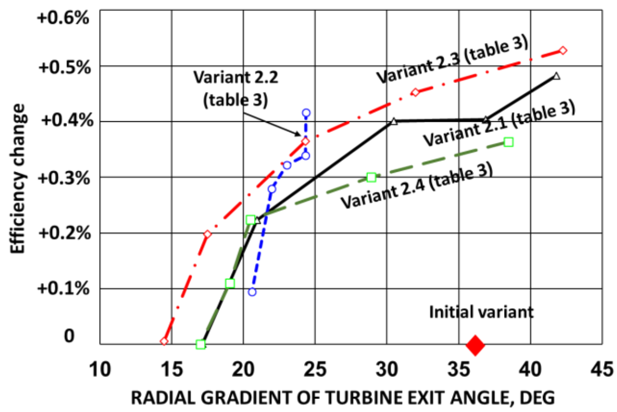

Figure 8. Comparison of the Pareto fronts of step 2 optimization problems.

From comparison of Pareto fronts of tasks 2.1, 2.3 and 2.5, it is obvious that results of the final statement of the problem 2D re-profiling of blades HPT (task 2.5) practically do not differ from results of solution of task 2.3. This testifies that change of thickness of profiles of blades RW practically had no influence on results of solution of the optimization problem.

VIII. Solving the Optimization Problems of Step 3

The turbine variants obtained as a result of solving the optimization problems of step 2 were used as input for solving the optimization problems of step 3. In this step, a change of their mutual position was added to the change of blades profiles. It was done by displacement of control points of the line connecting centres of gravity of control sections (blade skeleton line) in circumferential and axial directions (Fig. 9).

In step 3, two schemes were used to parameterize the shape of the line connecting the centres of gravity of the blade sections, shown in Fig. 10. In the first approach, the shape of the line was changed by shifting one of the four control points in circumfer-ential or axial direction. In the second approach, the shape of the line connecting the centres of gravity of the sections is described by the inclination angles of the three tangents to this line and the length of the central section (the same for offsets in both directions).

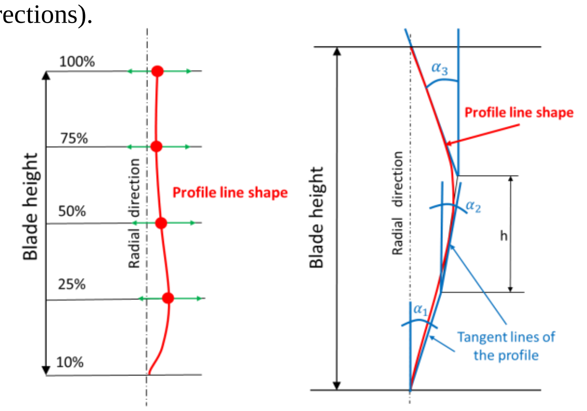

Figure 9. Parameterization schemes for blade cross-sections in axial and circumferential directions.

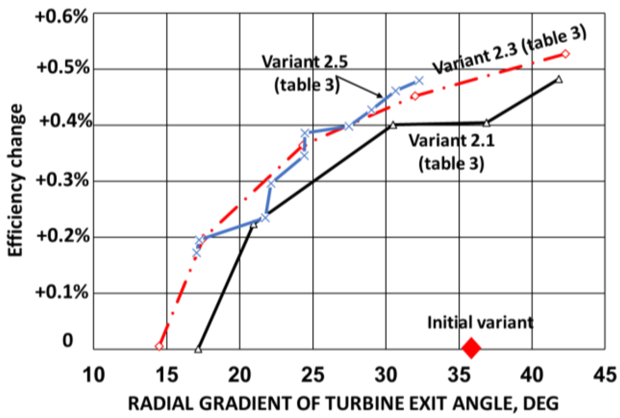

Figure 10. Comparison of the Pareto fronts of tasks 2.1, 2.3 and 2.5.

According to the results of solving the optimization problems of step 3, the best results were obtained in variant 3.2. For the obtained HPT variants, a comparison was made with the original version of the turbine, as well as with the best turbine variants obtained as a result of solving optimization problems of the second step on the verification numerical model (with a dense finite volume grid (27 thousand cells in the layer)).

According to the results of solving the optimization problems of step 3, the best results were obtained in variant 3.2. For the obtained HPT variants, a comparison was made with the original version of the turbine, as well as with the best turbine variants obtained as a result of solving optimization problems of the second step on the verification numerical model (with a dense finite volume grid (27 thousand cells in the layer)).

IX. Validation of Optimization Results

The results of the comparison of the obtained variants in terms of efficiency and gradient of the flow exit angle are shown in Fig. 11, and in terms of flow rate and pressure ratio in Fig. 12. The point numbers on the fronts are given in Fig. 11 and 12 for easy comparison of the results and they are identical.

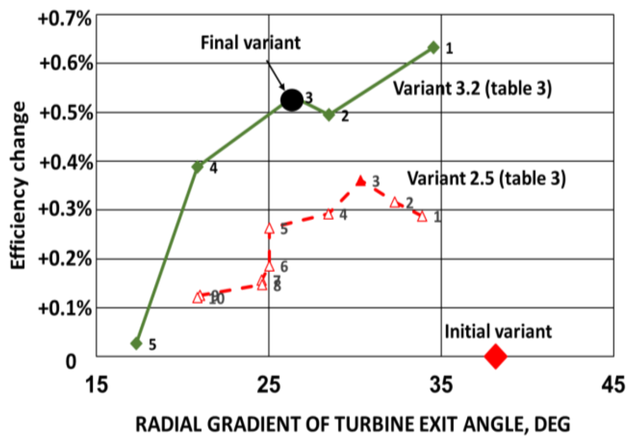

Figure 11. Comparison of best results of HPT optimisation steps 2 and 3 using a computational model with a dense finite volume grid.

In order to quantify the effect of re-profiling, graphs of the height distribution of energy losses for the nozzle guided vanes, shown in Fig. 13 and the rotor wheels, shown in Fig. 14, have been plotted.

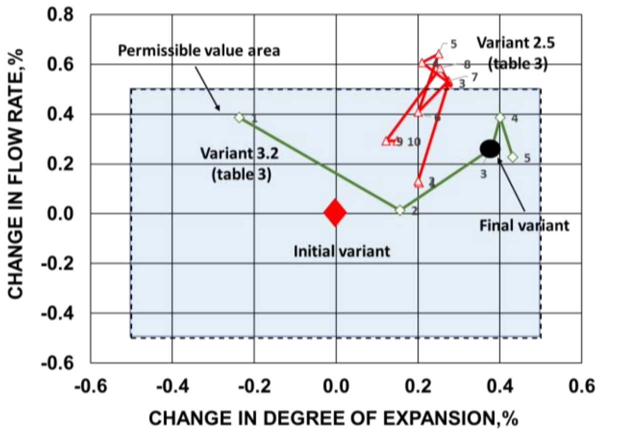

Figure 12. Comparison of best results of HPT optimization steps 2 and 3 using a computational model with a dense finite volume grid.

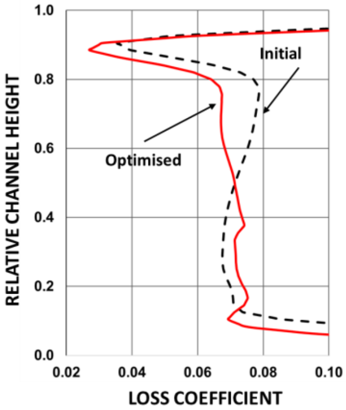

Figure 13. Comparison of NGV 1 height loss coefficient.

It can be seen from Figs. 13-16 that the optimization resulted in a significant (about 0.1) decrease in the Mach number in the 2nd CA stage, although a slight (about 0.05) increase in RW2 (resulting in a slightly higher loss factor in the middle part (Fig. 14)). In the 1st NGV stage, there was a reduction in the intensity of secondary streams at the periphery, which, together with some reduction in velocities, reduced the losses in the upper half of the blade.

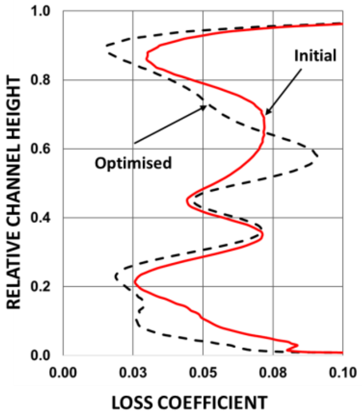

Figure 14. Comparison of NGV 2 height loss coefficient.

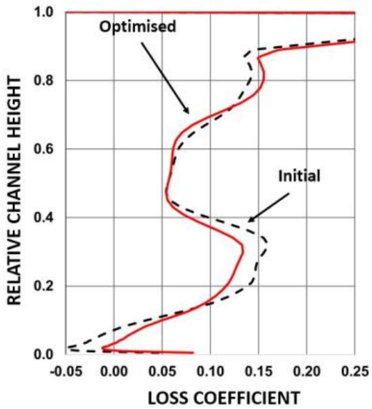

Figure 15. Comparison of RW1 height loss coefficient.

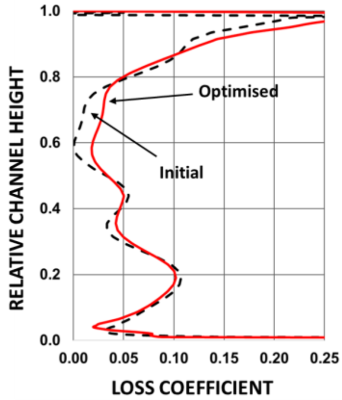

Figure 16. Comparison of RW2 height loss coefficient.

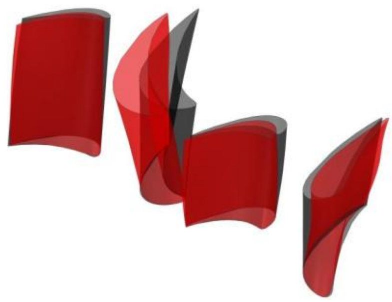

Figure 17. Comparison of blade shapes before and after optimisation (black-original, red – optimised).

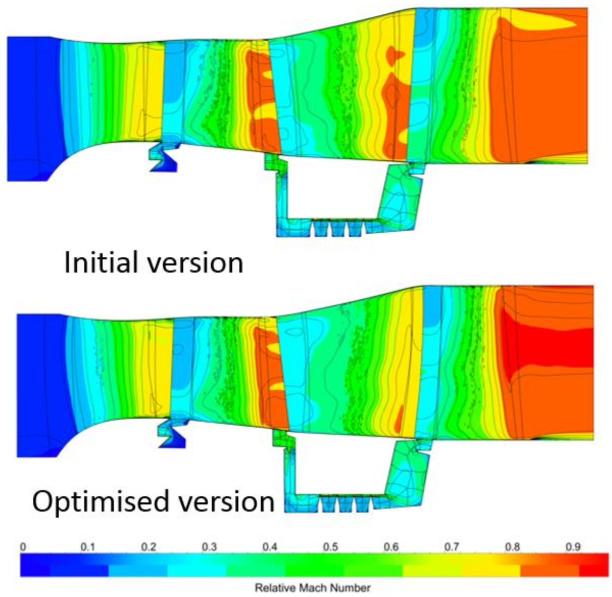

Figure 18. Comparison of mach number fields averaged in circumferential direction in the initial and optimised variants.

A decrease in the Mach number in the peripheral region in guide vanes channel and an increase in the Mach number in the peripheral region in the rotor blades channel indicates an increase in the degree of reactivity, which probably led to an increase in leaks through the radial clearance of the impellers, especially for the second stage rotor blades. Despite this, the overall reduction in losses in the turbine allowed to increase its efficiency and power.

X. CONCLUSION

In the work, the results of which are presented in the paper, the optimisation task of an axial two-stage cooled HPT was solved. The optimisation was carried out in a multi-criteria delivery. It looked for a solution with increased efficiency and reduced radial gradient of the outlet flow angle.

The initial turbine had a high efficiency and for this reason no significant improvement was found using conventional approaches. For this reason, a series of optimization tasks were solved in which the parametrization scheme, the number of sections to be changed, the finite volume grid and the degree of detail of the mathematical model were varied. As a result, a parametrization scheme with five parametric sections of NGV and three parametric sections of RW, as well as varying the thicknesses of profiles of NGV and RW blades sections was chosen.

The solution of HPT optimization tasks with two different schemes of parameterization of blade cross-section height alignment has been performed. Based on the results of problem solution the scheme of parameterization of blade cross sections height by three tangents was selected.

As a result of solving some optimization problems, including 2D and 3D re-profiling of blades, an increase in efficiency of 0.63% was obtained. In addition, a significant reduction in the unevenness of the flow at the turbine outlet was obtained, it allows to reduce losses in the transition channel between the high and low pressure turbines. A decrease in the Mach number in the nozzle devices of the first and second stages, which led to a decrease in losses is the reason for the increase in efficiency.

CONFLICT OF INTEREST

The authors declare no conflict of interest.

AUTHOR CONTRIBUTIONS

This work was carried out at the Samara National Research University named after S.P. Korolev in the interests of the leading Russian aircraft engine building company PJSC UEC Aviadvigatel. General management and coordination of work on the part of Samara University was carried out by Grigory Popov. He is also the author of the text of the article Evgeny Goryachkin directly formulated the optimization problem and executed it. The numerical models used in the optimization were developed by Vasily Zubanov. He, together with Anastasia Shcherban, processed the results of the calculation.

On the part of UEC Aviadvigatel PJSC, the work was supervised by Andrey Shvyrev. He provided the necessary information, provided experimental data and significantly influenced the formulation of the optimization problem, clarifying and concretizing the requirements of the customer.

REFERENCES

[1] M. P. Boyce, *Gas Turbine Engineering Handbook*, 10.1016/B978-0-7506-7846-9.X5000-7, 2006.

[2] A. Inozemtsev, V. Hairulin, A. Tihonov, and N. Samohvalov, “Improving design methodologies for modern gas turbines,” Bulletin of the Samara Aerospace University named after S. P. Koroleva, vol. 1, no. 5, pp. 139-147, 2014, (in Russian).

[3] F. Rasimarzabadi, R. Kamalimoghadam, M. Najafi, M. R. Mohammadi, and N. S. Fard, “Cool-ing improvement of gas turbine rotary blades,” in *Proc. the ASME Turbo Expo 2020: Turbomachinery Technical Conference and Exposition (GT2020)*, vol. 11, 2020.

[4] M. Zhang, N. Wang, A, F, Chen, and J. Han, "Influence of turbine blade leading edge profile on film cooling with shaped holes," in *Proc. the ASME Turbo Expo 2017: Turbomachinery Technical Conference and Exposition*, vol. 5C, Heat Transfer. Charlotte, North Carolina, USA. June 26–30, 2017, https://doi.org/10.1115/GT2017-63694

[5] C. C. Easterby, J. D. Moore, and D. G. Bogard, “CFD evaluation of internal flow effects on turbine blade leading-edge film cooling with shaped hole geometries,” in *Proc. the ASME Turbo Expo 2021: Turbomachinery Technical Conference and Exposition. Volume 5A: Heat Transfer — Combustors; Film Cooling*. Virtual, Online. June 7–11, 2021. https://doi.org/10.1115/GT2021-59780

[6] F. Wagner, A. Kuhhorn, T. Janetzke, and U. Gerstberger, “Multi-objective optimization of the cooling configuration of a high pressure turbine blade,” in *Proc. the ASME Turbo Ex-po 2018: Turbomachinery Technical Conference and Exposition*, vol. 5C. GT2018-75616, 2018.

[7] Y. Okita, T. Ideta, and S. Fujimoto, “Multi-objective shape optimization of arrowhead-shaped film cooling hole on transonic turbine blade,” in *Proc. ASME Turbo Expo 2020: Turbomachinery Technical Conference and Exposition*, vol. 7B. GT2020-14721 2020)

[8] K. Cremanns, D. Roos, A. Graßmann, “Sequential vs multidisciplinary coupled optimization and efficient surrogate modelling of a last stage and the successive axial radial diffuser in a low pressure steam turbine,” in *Proc. the ASME Turbo Expo 2014: Turbomachinery Technical Conference and Exposition*, vol. 2B. GT2014-25787, 2014.

[9] A. Châtel, T. Verstraete, G. Coussement, “Multipoint optimization of an axial turbine cas-cade using a hybrid algorithm,” in *Proc. the ASME Turbo Expo 2019: Turbomachin-ery Technical Conference and Exposition*, vol. 2D. GT2019-91471, 2019.

[10] JSC UEC-Aviadvigatel. [Online]. Available: https://avid.ru/en/, last accessed 2022/07/28.

[11] G. Popov, V. Matveev, O. Baturin, Y. Novikova, A. Volkov, “Selection of parameters for blade-to-blade finite-volume mesh for CFD simulation of axial turbines,” in *Proc. MATEC Web of Conferences*, vol. 220, 2018.

[12] Sigma Technology. [Online]. Available: https://www.iosotech.com/, last accessed 2022/07/28

[13] I. N. Egorov, G. V. Kretinin, I. A. Leshchenko, S. V. Kuptzov, “The main features of IOSO Technology usage for multi-objective design optimization,” in *Proc. 10th AIAA/ISSMO Multidisci-plinary Analysis and Optimisation Conference*, 2004.

[14] I. N. Egorov, G. V. Kretinin, I. A. Leshchenko, S. V. Kuptzov, “Multi-objective robust optimisation of air engine using IOSO technology,” in *Proc. the ASME Turbo Expo 2004: Power for Land, Sea, and Air*, vol. 2, Turbo Expo, pp. 157-163, 2004.

[15] E. Marchukov, I. Egorov, G. Popov, A. Salnikov, E. Goriachkin, D. Kolmakova, “Multi-disciplinary optimisation of the working process of uncooled axial turbine according to efficiency and strength criteria,” in *Proc. the ASME Turbo Expo 2017: Turbomachinery Technical Conference and Exposition*. vol. 2C: Turbomachinery, V02CT47A020, 2017.

[16] G. Popov, E. Goriachkin, I. Egorov, O. Baturin, A. Salnikov, A. Solovieva, Y. Zhurenkov, “Improvement of aerodynamic and strength characteristics of a multi-shaft axial turbine of a turboshaft engine,” in *Proc. the ASME Turbo Expo 2021:*

Turbomachinery Technical Conference and Exposition, Vol. 2D, 2021.

[17] G, Popov, E, Goriachkin, I, Egorov, O, Baturin, A, Salnikov, A, Solovieva, Y. Zhurenkov, "Improvement of aerodynamic and strength characteristics of a multi-shaft axial turbine of a turboshaft engine," in *Proc. the ASME Turbo Expo 2021: Turbomachinery Technical Conference and Exposition*, vol. 2D, 2021.

[18] Numeca AutoGrid Users Guide

Grigory Popov, Ph.D. Associate Professor of the Department of the Theory of Aircraft Engines, Samara National Research University named after S.P. Korolev. Specialist in numerical modeling and optimization of turbomachines. He graduated with honors from the specialty, master's and postgraduate studies of Samara University.

Vasily Zubanov, Ph.D. Associate Professor of the Department of the Theory of Aircraft Engines, Samara National Research University named after S.P. Korolev. Specialist in the numerical modeling and optimization of turbomachines, rocket engine workflow. Graduated from the specialty, magistracy and postgraduate studies of Samara University.

Evgeny Goryachkin, Ph.D. Associate Professor of the Department of the Theory of Aircraft Engines, Samara National Research University named after S.P. Korolev. Specialist in the numerical modeling and optimization of turbomachines. Graduated from the specialty, magistracy and postgraduate studies of Samara University.

Anstasia Shcherban, Engineer, Department of the Theory of Aircraft Engines, Samara National Research University named after S.P. Korolev. Specialist in the numerical modeling of turbomachines. Graduated from the specialty and postgraduate course of the Samara University.

Andrey Shvyrev is a leading specialist of PJSC "UEC Aviadvigatel" in the field of design, numerical and experimental research of turbines. The area of his scientific interests is aerodynamics and thermal state of aircraft engine turbines.